dent grain boundaries with $\Sigma > 50$ cannot be ruled out, but such high values of $\Sigma$ are of little or no physical significance. The axial ratios considered in this work, though they are approximations to the true $YBa_2Cu_3O_{7-\delta}$ structure, yield useful criteria for characterizing grain boundaries. Chisholm & Smith (1989), Babcock & Larbalestier (1989) and Babcock (1988) have observed grain-boundary-dislocation networks. Babcock (1988) has speculated on the possibility of these structures being related to CSL structures.

### Concluding remarks

Consideration of the geometrical structure of grain boundaries can provide a valuable insight into the properties of materials. We have presented here a method to determine the geometry of grain boundaries in tetragonal and near-tetragonal orthorhombic crystal systems, with particular emphasis on $YBa_2Cu_3O_{7-\delta}$. Data on the possible grain-boundary structures of $YBa_2Cu_3O_{7-\delta}$ are presented. It is hoped that this will aid in characterizing the grain-boundary structures observed in $YBa_2Cu_3O_{7-\delta}$.

This work was supported by the National Science Foundation, under grant No. DMR-8901994. NC also received support from the US Department of Energy, through contract No. DE-AC-87CH00016. We would like to thank the referees for many helpful suggestions, and for drawing our attention to the work of Grimmer and Erochine *et al.*

### References

BABCOCK, S. E. (1988). *EMSA Proc.* pp. 622–623.
BABCOCK, S. E. & LARBALESTIER, D. C. (1989). *J. Mater. Res.* Submitted.
BONNET, R. (1981). *Acta Cryst.* A**27**, 184–189.
CHEN, F. R. & KING, A. H. (1987). *Acta Cryst.* B**43**, 416–422.
CHEN, F. R. & KING, A. H. (1988). *Philos. Mag. A*, **57**, 431–455.
CHISHOLM, M. F. & SMITH, D. A. (1989). *Philos. Mag. A*, **59**(2), 181–197.
EROCHINE, S. & NOUET, G. (1983). *Scr. Metall.* **17**, 1069–1072.
GRIMMER, H. (1980). *Acta Cryst.* A**36**, 382–389.
GRIMMER, H. & WARRINGTON, D. H. (1987). *Acta Cryst.* A**43**, 232–243.
JOHNSTON, D. C. (1987). *Chemistry of High Temperature Superconductors*, ACS Symposium Series 351, pp. 136–151. Washington, DC: American Chemical Society.
KING, A. H. (1982). *Acta Metall.* **30**, 419–427.
KING, A. H. & SMITH, D. A. (1980). *Acta Cryst.* A**36**, 335–343.

*Acta Cryst.* (1990). B**46**, 125–131

# Structural Study of the Phase Transition of $Na_4Ca_4[Si_6O_{18}]$

BY HITOSHI OHSATO* AND YOSHIO TAKÉUCHI

*Mineralogical Institute, Faculty of Science, University of Tokyo, Hongo, Tokyo* 113, *Japan*

AND IWAO MAKI

*Department of Materials Science and Engineering, Nagoya Institute of Technology, Gokiso-cho, Showa-ku, Nagoya* 466, *Japan*

(*Received* 30 *June* 1989; *accepted* 26 *September* 1989)

### Abstract

The structure of $Na_4Ca_4[Si_6O_{18}]$, which undergoes a reversible phase transition at 748 K, has been studied by means of X-ray single-crystal diffraction at 993, 888, 773, 738, 643 and 523 K. The crystal data of the high-temperature modification at 773 K are: $M_r = 708{\cdot}8$, trigonal, $R\bar{3}m$, $a_R = 7{\cdot}519$ Å, $\alpha = 89{\cdot}22°$, $Z = 1$; $a_H = 10{\cdot}561$ (1), $c_H = 13{\cdot}199$ (3) Å, $V_H = 1274{\cdot}9$ Å$^3$, $Z = 3$, $D_x = 2{\cdot}77$ Mg m$^{-3}$, $\lambda$(Mo $K\alpha$) = 0·71073 Å, $\mu = 1{\cdot}89$ mm$^{-1}$, $F(000) = 1056$, $R = 0{\cdot}047$ for 599 observed reflections ($F_{obs} > 3\sigma$). The high-temperature form, made up of puckered six-membered $[Si_6O_{18}]^{12-}$ rings, is isostructural with $Na_6Ca_3[Si_6O_{18}]$. One of the cation sites is only partly occupied by Na ions with the remainder vacant. In the low-temperature form the vacancies are clustered to produce a specific vacant cation site. The vacancies, in both forms, can accommodate additional Na ions with the replacement of Ca by 2Na and thus play an essential role in the formation of continuous solid solutions as represented by $Na_{4+2x}Ca_{4-x}[Si_6O_{18}]$ $(0 \le x \le 1)$. The difference in structure between the high- and low-temperature forms is described in terms of their cation coordination polyhedra and configurations of the $[Si_6O_{18}]^{12-}$ ring.

* Present address: Department of Materials Science and Engineering, Nagoya Institute of Technology, Gokiso-cho, Showa-ku, Nagoya 466, Japan.

0108-7681/90/020125-07$03.00 

## Introduction

Three metasilicates, $Na_4Ca_4[Si_6O_{18}]$, $Na_6Ca_3[Si_6O_{18}]$ and $Na_8Ca_2[Si_6O_{18}]$, occur as distinct ternary compounds in the system $Na_2O$–$CaO$–$SiO_2$. The structures of $Na_4Ca_4[Si_6O_{18}]$ and $Na_6Ca_3[Si_6O_{18}]$ at 298 K have been determined by Ohsato, Maki & Takéuchi (1985) and Ohsato, Takéuchi & Maki (1986), and those of natural analogues of these compounds by Fischer & Tillmanns (1983, 1987). The structures consist of puckered six-membered rings of silicate tetrahedra, which are stacked in a cubic close-packing arrangement and held together by alkali and alkaline-earth ions. In the structure of $Na_8Ca_2[Si_6O_{18}]$ a ring configuration consisting of 12 silicate tetrahedra has been found by Fischer & Tillmanns (1984).

$Na_4Ca_4[Si_6O_{18}]$ undergoes a reversible phase transition at around 758 K (Maki & Sugimura, 1968). At elevated temperature an isomorphous solid-solution series is formed between $Na_4Ca_4[Si_6O_{18}]$ and $Na_6Ca_3[Si_6O_{18}]$ with the replacement of Ca by 2Na; *i.e.*, the chemical formula of the series can be represented by $Na_{4+2x}Ca_{4-x}[Si_6O_{18}]$ ($0 \le x \le 1$). The high–low inversion was observed for the solid solutions with $x$ up to 0·5; the transition temperature, $T_c$, lowers with increasing $x$ (Maki & Sugimura, 1968).

We have studied the structure of $Na_4Ca_4[Si_6O_{18}]$ at elevated temperatures in order to elucidate the structural mechanism of this phase transition.

## Experimental

Crystals of $Na_4Ca_4[Si_6O_{18}]$ were prepared as reported previously (Ohsato, Takéuchi & Maki, 1986). A suitable single crystal was shaped into a sphere ($r \simeq$ 0·159 mm) using the Bond method (1951) and sealed in a capillary made of silica glass. Intensity data were collected on a four-circle X-ray single-crystal diffractometer (Rigaku AFC-5). An electric resistance furnace of the horseshoe type as described by Brown, Sueno & Prewitt (1973) was fitted to the $\chi$ circle on the opposite side of the goniometer head. The thermocouple for temperature control was fixed 2 mm away from the crystal. The temperature was calibrated by reading another thermocouple placed at exactly the same position as the crystal. The cell dimensions (Table 1) were determined at each temperature by the least-squares method from $\sin 2\theta$ values of 25 reflections in the range $20 < 2\theta < 30°$.

The $\omega$–$2\theta$ scan technique was adopted to collect diffraction intensity data with graphite-monochromatized Mo $K\alpha$ radiation. Intensity data were collected at 993, 888 and 773 K for the high-temperature form and at 738, 643 and 523 K for the low-temperature form. Three standard reflections showed no significant change during the measurements at each temperature. The intensity data were corrected for Lorentz and polarization factors. Because of the small $\mu r$ (~0·299) no correction was made for absorption. The intensity-measurement conditions are summarized in Table 1.

The atomic parameters of the low-temperature form at 298 K (Ohsato, Takéuchi & Maki, 1986) served to provide initial atomic parameters for the present study. Atomic scattering factors for $O^{2-}$ were those given by Tokonami (1965) and those for other ions, as well as $f'$ and $f''$ values, were from *International Tables for X-ray Crystallography* (1974). Full-matrix least-squares refinement on $F$ of atomic parameters, with anisotropic thermal parameters and occupancies for Na and Ca atoms, was carried out with the program *RADY* (Busing, Martin & Levy, 1963). The calculations were carried out on a HITAC M-280H computer of the University of Tokyo. The Na/Ca ratio of the crystal obtained by the structure analysis was in accord with the formula $Na_4Ca_4[Si_6O_{18}]$ within the limits of error, so that in the subsequent refinement the ratio was fixed to 1.

## Results and discussion

### *Crystal data*

High-temperature form at 773 K: $M_r = 708·8$, trigonal, $R\bar{3}m$, $a_R = 7·519$ Å, $\alpha = 89·22°$, $Z = 1$; $a_H = 10·561$ (1), $c_H = 13·199$ (3) Å, $V_H = 1274·9$ Å$^3$, $Z = 3$, $D_x = 2·77$ Mg m$^{-3}$.

Low-temperature form at 298 K (Ohsato, Takéuchi & Maki, 1986): trigonal, $P3_121$ (or $P3_221$), $a_H = 10·464$ (2), $c_H = 13·168$ (2) Å, $V_H = 1248·7$ Å$^3$, $Z = 3$, $D_m = 2·817$, $D_x = 2·829$ Mg m$^{-3}$.

### *Change of cell dimensions with temperature*

In order to confirm the transition temperature, $T_c$, diffraction intensity variation with temperature was followed for the 120, 123 and $\bar{4}\bar{2}4$ reflections around $T_c$ (indices referred to the trigonal cell). The 120 and 123 reflections with $-h + k + l \neq 3n$ disappeared just above $T_c$ and reappeared below this temperature, whereas the reflection $\bar{4}\bar{2}4$ with $-h + k + l = 3n$ persisted above $T_c$. These changes correspond to the reported space-group change from $R\bar{3}m$ to $P3_121$ in the cooling cycle. The transition temperature thus determined was 748 K, which agrees well with the temperature (758 K) given by Maki & Sugimura (1968).

Fig. 1 shows the variations of cell dimensions and cell volumes with temperature. The $a$ axis exhibits an abrupt expansion (0·27%) at $T_c$ while the $c$ axis contracts by 0·06%. This change shows a feature of the first-order phase transition. The thermal-expansion coefficient along the $c$ axis is $7·86 \times 10^{-6}$ K$^{-1}$ for the high-temperature form and $6·17 \times$

Table 1. *Intensity-measurement data and cell dimensions at each temperature*

| | 993 K | 888 K | 773 K | 738 K | 643 K | 523 K |
|---|---|---|---|---|---|---|
| No. of reflections for cell-dimension determination | 25 | 25 | 25 | 25 | 25 | 25 |
| $\theta$ range (°) | 12–14 | 12–14 | 12–14 | 12–14 | 12–14 | 12–14 |
| No. of reflections measured | 740 | 731 | 729 | 2185 | 2175 | 2169 |
| *hkl* range *h* | 0–13 | 0–13 | 0–14 | 0–14 | 0–14 | 0–14 |
| *k* | 0–13 | 0–13 | 0–14 | 0–14 | 0–14 | 0–14 |
| *l* | 0–20 | 0–20 | 0–21 | 0–21 | 0–21 | 0–21 |
| $(\sin\theta/\lambda)_{max}$ (Å$^{-1}$) | 0·807 | 0·807 | 0·807 | 0·807 | 0·807 | 0·807 |
| No. of unique reflections | 720 | 712 | 710 | 2106 | 2094 | 2087 |
| No. of reflections $> 3\sigma(\|F_o\|)$ | 584 | 593 | 599 | 1711 | 1792 | 1792 |
| $\Delta\rho$ (e Å$^{-3}$) on difference Fourier map | ± 0·6 | ± 0·6 | ± 0·6 | ± 1·2 | ± 1·1 | ± 1·3 |
| $(\Delta/\sigma)_{max}$ on least-squares refinement | 0·53 | 0·69 | 0·64 | 0·53 | 0·69 | 0·64 |
| $G_{iso}$ ($\times 10^5$) | — | — | — | 1·41 | 1·56 | 1·63 |
| $R$ (%) | 5·18 | 5·09 | 4·76 | 4·60 | 3·97 | 3·57 |
| $wR$ (%) | 5·28 | 5·35 | 4·90 | 4·38 | 3·92 | 3·72 |
| Cell dimensions $a_H$ (Å) | 10·588 (1) | 10·574 (1) | 10·561 (1) | 10·530 (1) | 10·513 (1) | 10·494 (1) |
| $c_H$ (Å) | 13·222 (2) | 13·209 (1) | 13·199 (3) | 13·203 (2) | 13·195 (2) | 13·189 (3) |
| $V_x$ (Å$^3$) | 1283·6 (3) | 1279·0 (3) | 1274·9 (3) | 1267·9 (2) | 1263·0 (2) | 1257·8 (3) |
| $D_x$ (Mg m$^{-3}$) | 2·755 | 2·766 | 2·774 | 2·790 | 2·800 | 2·812 |

$10^{-6}$ K$^{-1}$ for the low-temperature form. Along the *a* axis the thermal-expansion coefficient of the high-temperature form is $11{\cdot}6 \times 10^{-6}$ K$^{-1}$ and that of the low-temperature form is $14{\cdot}2 \times 10^{-6}$ K$^{-1}$. These coefficients are relatively small, particularly along the *c* axis, and comparable with those of quartz, which are $9 \times 10^{-6}$ and $14 \times 10^{-6}$ K$^{-1}$ along the *c* and *a* axes, respectively (Taylor, 1984). Thermal expansion is much less in the direction perpendicular to the plane including the bridging O atoms of the $[Si_6O_{18}]^{12-}$ ring than in the direction parallel to it. Similar phenomena have been observed in some ring silicates; *e.g.*, cordierite (Ikawa, Otagiri, Imai, Suzuki, Urabe & Udagawa, 1986).

*Structure of the high-temperature form*

Tables 2 and 3* give the final atomic parameters and $B_{eq}$'s, and the bond lengths at each temperature, respectively. The high-temperature form (Fig. 2) is isostructural with $Na_6Ca_3[Si_6O_{18}]$ (Ohsato, Maki & Takéuchi, 1985) and very similar in structure to the low-temperature form of $Na_4Ca_4[Si_6O_{18}]$ (Ohsato, Takéuchi & Maki, 1986), but its $[Si_6O_{18}]^{12-}$ ring is expanded and has point symmetry $\bar{3}m$, as will be discussed later. The structure can best be described by reference to a one-octant cell with half the cell edge length of the rhombohedral cell and the origin at $\frac{1}{4},\frac{1}{4},\frac{1}{4}$. The direction [111] of such a subcell is parallel to *c* of the trigonal cell. The six Si atoms of one $[Si_6O_{18}]^{12-}$ ring basically define the corners of the subcell. The other two corners of the subcell, existing on the threefold axis and designated as $M(1)$, are occupied by cations. No cations are found in the centre of such a subcell. The other cation sites [$M(2)$, $M(3)$, $M(4)$] lie near the centres of the neighbouring subcells. Thus cations in these three sites are located at the corners and the centres of the edges and faces of the rhombohedral unit cell (Fig. 2).

In the low-temperature form, the cationic vacancies introduced with the substitution scheme, $2Na \rightleftarrows Ca$, occur exclusively at $M(22)$ (Ohsato, Takéuchi & Maki, 1986). In the structure analysis of the high-temperature form such cationic vacancies were allocated to the $M(2)$ site. It has been found that one-third of the $M(2)$ site is vacant, the remainder being occupied by Na. The reinvestigation of the structure of mineral combeite has revealed that 24% of the $M(2)$ site in $Na_{2\cdot4}Ca_{1\cdot5}(Fe,Mn,Mg,Zn)_{0\cdot3}Si_3O_9$ ($R\bar{3}m$) is vacant and 60% of the $M(22)$ site in $Na_{2\cdot2}Ca_{1\cdot9}Si_3O_9$ ($P3_121$) is vacant (Fischer & Tillmanns, 1987); these compounds correspond to the high- and low-temperature modifications of $Na_4Ca_4[Si_6O_{18}]$, respectively.

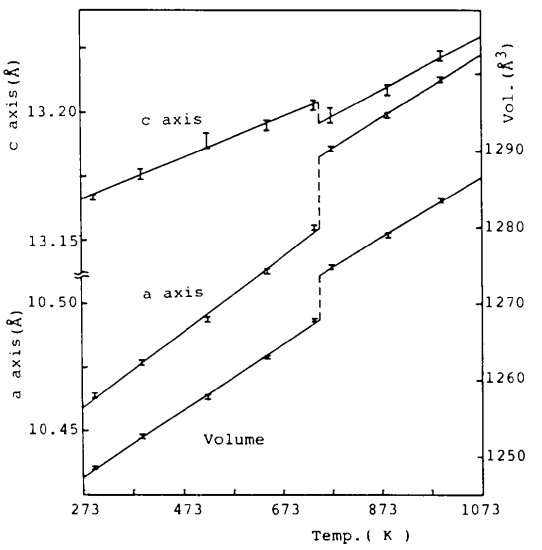


Fig. 1. Variation in cell dimensions ($a_H$, $c_H$) and volume of the trigonal cell as a function of temperature. Vertical lines give e.s.d.'s.

* Lists of structure factors, anisotropic thermal parameters and bond lengths and angles have been deposited with the British Library Document Supply Centre as Supplementary Publication No. SUP 52374 (27 pp.). Copies may be obtained through The Technical Editor, International Union of Crystallography, 5 Abbey Square, Chester CH1 2HU, England.

Table 2. *Atomic coordinates* ($\times 10^4$) *and equivalent isotropic temperature factors* ($Å^2$) *at each temperature*

$$B_{eq} = (1/3)\sum_i\sum_j B_{ij}a_i^*a_j^*\mathbf{a}_i.\mathbf{a}_j.$$

(*a*) High-temperature form (origin at $\bar{3}m$)

| Position and occupancy | | | 993 K | 888 K | 773 K |
|---|---|---|---|---|---|
| O(1) 18(*g*) | | *x* | 2474 (5) | 2476 (5) | 2483 (5) |
| | | $B_{eq}$ | 5·0 (3) | 4·7 (2) | 4·6 (2) |
| O(2) 18(*h*) | | *x* | 1188 (3) | 1186 (3) | 1183 (2) |
| | | *z* | 6727 (3) | 6729 (3) | 6730 (2) |
| | | $B_{eq}$ | 4·19 (3) | 3·93 (3) | 3·72 (2) |
| O(3) 18(*h*) | | *x* | 2371 (2) | 2371 (2) | 2372 (2) |
| | | *z* | 5497 (3) | 5500 (3) | 5502 (3) |
| | | $B_{eq}$ | 3·89 (5) | 3·62 (4) | 3·57 (4) |
| Si 18(*h*) | | *x* | 1506 (1) | 1506 (1) | 1507 (1) |
| | | *z* | 5622 (1) | 5623 (1) | 5625 (1) |
| | | $B_{eq}$ | 1·71 (1) | 1·557 (9) | 1·509 (9) |
| *M*(1) 6(*c*) | | *z* | 2575 (3) | 2569 (2) | 2565 (2) |
| 0·57 (1) Na | | $B_{eq}$ | 3·75 (8) | 3·35 (7) | 3·04 (6) |
| 0·43 (1) Ca | | | | | |
| *M*(2) 9(*e*) | | $B_{eq}$ | 5·6 (4) | 5·1 (4) | 4·6 (3) |
| 0·67 (1) Na | | | | | |
| 0·33 Vacancy | | | | | |
| *M*(3) 9(*d*) | | $B_{eq}$ | 3·8 (4) | 3·5 (3) | 3·3 (3) |
| 0·29 (1) Na | | | | | |
| 0·71 (1) Ca | | | | | |
| *M*(4) 3(*a*) | | $B_{eq}$ | 2·25 (5) | 2·04 (5) | 1·96 (4) |
| 1·0 Ca | | | | | |

(*b*) Low-temperature form* (origin at $3_121$)

| Position and occupancy | | | 738 K | 643 K | 523 K |
|---|---|---|---|---|---|
| O(11) 3(*b*) | | *x* | 1521 (9) | 1590 (6) | 1635 (5) |
| | | $B_{eq}$ | 4·0 (4) | 3·0 (3) | 2·2 (2) |
| O(12) 3(*b*) | | *x* | 5600 (9) | 5580 (7) | 5573 (6) |
| | | $B_{eq}$ | 3·5 (4) | 3·0 (3) | 2·7 (3) |
| O(13) 6(*c*) | | *x* | 3437 (5) | 3442 (4) | 3447 (4) |
| | | *y* | 2762 (6) | 2790 (4) | 2818 (4) |
| | | *z* | 8354 (3) | 8363 (3) | 8371 (2) |
| | | $B_{eq}$ | 2·3 (2) | 1·9 (1) | 1·6 (1) |
| O(14) 6(*c*) | | *x* | 5850 (7) | 5854 (5) | 5854 (4) |
| | | *y* | 2611 (7) | 2627 (5) | 2636 (4) |
| | | *z* | 8240 (4) | 8226 (3) | 8219 (3) |
| | | $B_{eq}$ | 2·8 (2) | 2·3 (1) | 1·8 (1) |
| O(21) 6(*c*) | | *x* | 2387 (6) | 2420 (5) | 2436 (4) |
| | | *y* | 1457 (6) | 1490 (5) | 1512 (4) |
| | | *z* | 6618 (3) | 6623 (2) | 6625 (2) |
| | | $B_{eq}$ | 2·6 (2) | 2·2 (1) | 1·8 (1) |
| O(22) 6(*c*) | | *x* | 4712 (8) | 4747 (6) | 4771 (5) |
| | | *y* | 2469 (5) | 2479 (5) | 2482 (4) |
| | | *z* | 33 (3) | 32 (2) | 31 (2) |
| | | $B_{eq}$ | 2·9 (2) | 2·4 (1) | 2·0 (1) |
| O(23) 6(*c*) | | *x* | 5578 (5) | 5551 (4) | 5533 (4) |
| | | *y* | 1133 (8) | 1123 (6) | 1117 (5) |
| | | *z* | 6563 (3) | 6561 (2) | 6553 (2) |
| | | $B_{eq}$ | 2·9 (1) | 2·6 (1) | 2·2 (1) |
| O(31) 6(*c*) | | *x* | 720 (5) | 694 (4) | 673 (3) |
| | | *y* | 1959 (5) | 1914 (4) | 1881 (4) |
| | | *z* | 7934 (3) | 7941 (3) | 7945 (2) |
| | | $B_{eq}$ | 2·3 (2) | 1·8 (1) | 1·47 (9) |
| O(32) 6(*c*) | | *x* | 5910 (6) | 5937 (5) | 5950 (4) |
| | | *y* | 4929 (4) | 4955 (4) | 4975 (3) |
| | | *z* | 8869 (3) | 8874 (3) | 8878 (2) |
| | | $B_{eq}$ | 2·6 (1) | 2·3 (1) | 1·9 (1) |
| O(33) 6(*c*) | | *x* | 8000 (4) | 7993 (4) | 7989 (3) |
| | | *y* | 2199 (7) | 2192 (5) | 2177 (4) |
| | | *z* | 7785 (3) | 7775 (3) | 7769 (2) |
| | | $B_{eq}$ | 2·5 (1) | 2·1 (1) | 1·8 (1) |
| Si(1) 6(*c*) | | *x* | 1958 (2) | 1975 (1) | 1981 (1) |
| | | *y* | 1524 (2) | 1528 (1) | 1524 (1) |
| | | *z* | 7766 (1) | 7773 (1) | 7777 (1) |
| | | $B_{eq}$ | 1·17 (4) | 1·01 (3) | 0·83 (3) |
| Si(2) 6(*c*) | | *x* | 4967 (2) | 4979 (2) | 4993 (1) |
| | | *y* | 3192 (1) | 3212 (1) | 3226 (1) |
| | | *z* | 8956 (1) | 8956 (1) | 8957 (1) |
| | | $B_{eq}$ | 1·24 (3) | 1·09 (3) | 0·93 (3) |
| Si(3) 6(*c*) | | *x* | 6264 (1) | 6254 (1) | 6248 (1) |
| | | *y* | 1486 (2) | 1481 (2) | 1485 (1) |
| | | *z* | 7656 (1) | 7649 (1) | 7643 (1) |
| | | $B_{eq}$ | 1·18 (3) | 1·04 (3) | 0·86 (2) |
| *M*(1) 6(*c*) | | *x* | 3133 (2) | 3107 (2) | 3092 (2) |
| 0·57 (1) Na | | *y* | −138 (2) | −159 (2) | −168 (2) |
| 0·43 (1) Ca | | *z* | 5905 (1) | 5903 (1) | 5899 (1) |
| | | $B_{eq}$ | 1·93 (6) | 1·54 (5) | 1·15 (4) |
| *M*(1′)† 6(*c*) | | *x* | 2790 (30) | 2780 (20) | 2790 (10) |
| 0·57 (1) Na | | *y* | −290 (20) | −300 (10) | −310 (10) |

Table 2 (*cont.*)

| Position and occupancy | | 738 K | 643 K | 523 K |
|---|---|---|---|---|
| 0·43 (1) Ca | *z* | 6260 (20) | 6230 (10) | 6200 (10) |
| | $B_{eq}$ | 8·3 (1) | 6·4 (6) | 5·0 (4) |
| *M*(21) 6(*c*) | *x* | 5042 (6) | 5040 (4) | 5039 (4) |
| 1·0 Na | *y* | 3368 (4) | 3369 (4) | 3372 (3) |
| | *z* | 6642 (2) | 6641 (2) | 6640 (2) |
| | $B_{eq}$ | 4·0 (1) | 3·35 (8) | 2·73 (6) |
| *M*(22)‡ 3(*a*) | *x* | 1630 | 1630 | 1630 |
| *M*(31) 6(*c*) | *x* | 5184 (3) | 5217 (2) | 5241 (2) |
| 0·43 (1) Na | *y* | 3594 (3) | 3643 (2) | 3681 (2) |
| 0·57 (1) Ca | *z* | 1593 (1) | 1581 (1) | 1569 (1) |
| | $B_{eq}$ | 3·35 (7) | 2·89 (5) | 2·41 (4) |
| *M*(32) 3(*b*) | *x* | 8254 (3) | 8236 (2) | 8222 (1) |
| 1·0 Ca | $B_{eq}$ | 2·02 (6) | 1·65 (5) | 1·28 (4) |
| *M*(4) 3(*a*) | *x* | 3108 (1) | 3080 (1) | 3059 (1) |
| 1·0 Ca | $B_{eq}$ | 1·49 (5) | 1·27 (4) | 1·05 (3) |

* See previous paper (Ohsato, Takéuchi & Maki, 1986) for the room-temperature data.

† $M(1')/[M(1) + M(1')]$ is *ca* 0·25.

‡ *M*(22) is vacant and the coordinates are only approximate.

Table 3. *Selected bond lengths* (Å) *at each temperature*

(*a*) High-temperature form

| | 993 K | 888 K | 773 K |
|---|---|---|---|
| Si—O(1) × 2 | 1·623 (1) | 1·623 (1) | 1·623 (1) |
| Si—O(2) | 1·573 (4) | 1·574 (4) | 1·575 (3) |
| Si—O(3) | 1·594 (2) | 1·593 (2) | 1·591 (2) |
| Mean | 1·603 (2) | 1·603 (2) | 1·603 (2) |
| *M*(1)—O(2$^{i}$) × 3 | 2·367 (3) | 2·362 (3) | 2·355 (2) |
| *M*(1)—O(3$^{vi}$) × 3 | 2·563 (3) | 2·556 (3) | 2·551 (4) |
| Mean | 2·465 (3) | 2·459 (3) | 2·453 (3) |
| *M*(2)—O(1$^{iv}$) × 4 | 2·682 (1) | 2·679 (2) | 2·676 (1) |
| *M*(2)—O(2$^{vi}$) × 4 | 2·727 (3) | 2·722 (3) | 2·718 (2) |
| Mean | 2·704 (2) | 2·701 (3) | 2·697 (1) |
| *M*(3)—O(1) × 2 | 2·674 (6) | 2·669 (6) | 2·658 (5) |
| *M*(3)—O(2$^{vi}$) × 2 | 2·297 (3) | 2·295 (3) | 2·293 (3) |
| *M*(3)—O(3) × 4 | 2·738 (2) | 2·735 (2) | 2·732 (2) |
| Mean | 2·612 (3) | 2·608 (3) | 2·604 (3) |
| *M*(4)—O(3$^{vi}$) × 6 | 2·347 (3) | 2·341 (3) | 2·335 (3) |

Symmetry operations: (i) $-x, -y, -z$; (iv) $\frac{1}{3}-y, \frac{2}{3}+x-y, \frac{2}{3}+z$; (vi) $\frac{1}{3}-x, \frac{2}{3}-y, \frac{2}{3}-z$.

(*b*) Low-temperature form*

| | 738 K | 643 K | 523 K |
|---|---|---|---|
| Si(1)—O(11) | 1·615 (3) | 1·625 (2) | 1·627 (2) |
| Si(1)—O(13) | 1·643 (4) | 1·644 (3) | 1·653 (3) |
| Si(1)—O(21) | 1·592 (5) | 1·593 (4) | 1·594 (3) |
| Si(1)—O(31) | 1·599 (7) | 1·605 (5) | 1·609 (5) |
| Mean | 1·612 (5) | 1·617 (4) | 1·621 (3) |
| Si(2)—O(13) | 1·645 (5) | 1·644 (4) | 1·648 (4) |
| Si(2)—O(14) | 1·643 (8) | 1·648 (6) | 1·645 (5) |
| Si(2)—O(22) | 1·571 (4) | 1·575 (4) | 1·578 (3) |
| Si(2)—O(32) | 1·590 (4) | 1·593 (3) | 1·594 (3) |
| Mean | 1·612 (5) | 1·615 (4) | 1·617 (4) |
| Si(3)—O(12) | 1·626 (2) | 1·624 (1) | 1·629 (1) |
| Si(3)—O(14) | 1·646 (8) | 1·648 (6) | 1·645 (5) |
| Si(3)—O(23) | 1·573 (4) | 1·572 (4) | 1·578 (3) |
| Si(3)—O(33) | 1·601 (5) | 1·601 (4) | 1·602 (3) |
| Mean | 1·611 (5) | 1·611 (4) | 1·614 (3) |
| *M*(1)—O(21) | 2·376 (8) | 2·384 (6) | 2·389 (5) |
| *M*(1)—O(22$^{v}$) | 2·351 (6) | 2·347 (5) | 2·346 (4) |
| *M*(1)—O(23) | 2·393 (5) | 2·389 (4) | 2·381 (4) |
| *M*(1)—O(31$^{iii}$) | 2·470 (4) | 2·461 (3) | 2·454 (3) |
| *M*(1)—O(32$^{iv}$) | 2·513 (6) | 2·501 (5) | 2·491 (4) |
| *M*(1)—O(33$^{iii}$) | 2·735 (5) | 2·758 (4) | 2·765 (3) |
| Mean | 2·473 (6) | 2·473 (5) | 2·471 (4) |
| *M*(1′)—O(11) | 3·132 (5) | 3·126 (3) | 3·141 (2) |
| *M*(1′)—O(21) | 2·139 (8) | 2·158 (6) | 2·199 (5) |
| *M*(1′)—O(22$^{v}$) | 2·126 (6) | 2·145 (5) | 2·139 (4) |
| *M*(1′)—O(23) | 2·576 (5) | 2·561 (4) | 2·533 (4) |
| *M*(1′)—O(31$^{iii}$) | 2·629 (4) | 2·598 (3) | 2·587 (2) |
| *M*(1′)—O(32$^{iv}$) | 3·000 (5) | 2·958 (4) | 2·909 (4) |
| *M*(1′)—O(33$^{iii}$) | 3·180 (4) | 3·169 (3) | 3·157 (3) |
| Mean | 2·683 (5) | 2·674 (4) | 2·666 (3) |

Table 3 (*cont.*)

| | 738 K | 643 K | 523 K |
|---|---|---|---|
| *M*(21)—O(12$^{iii}$) | 2·659 (8) | 2·656 (6) | 2·651 (6) |
| *M*(21)—O(13) | 2·702 (6) | 2·708 (5) | 2·714 (4) |
| *M*(21)—O(14) | 2·548 (8) | 2·527 (6) | 2·515 (5) |
| *M*(21)—O(14$^{iii}$) | 2·777 (6) | 2·796 (5) | 2·806 (4) |
| *M*(21)—O(21) | 2·498 (7) | 2·459 (5) | 2·437 (4) |
| *M*(21)—O(22$^{iii}$) | 2·547 (5) | 2·516 (4) | 2·491 (3) |
| *M*(21)—O(23) | 2·683 (11) | 2·672 (9) | 2·667 (7) |
| *M*(21)—O(23$^{iii}$) | 2·695 (8) | 2·687 (6) | 2·678 (5) |
| Mean | 2·639 (7) | 2·628 (6) | 2·620 (5) |
| *M*(31)—O(13') | 2·473 (7) | 2·453 (5) | 2·431 (5) |
| *M*(31)—O(14$^{ii}$) | 2·529 (8) | 2·514 (6) | 2·507 (5) |
| *M*(31)—O(22) | 2·304 (5) | 2·305 (4) | 2·307 (4) |
| *M*(31)—O(23$^{iii}$) | 2·289 (4) | 2·295 (4) | 2·291 (3) |
| *M*(31)—O(32$^{ii}$) | 2·811 (4) | 2·835 (3) | 2·862 (3) |
| *M*(31)—O(32') | 2·655 (8) | 2·630 (6) | 2·599 (5) |
| *M*(31)—O(33$^{ii}$) | 2·642 (5) | 2·603 (4) | 2·581 (3) |
| Mean | 2·529 (6) | 2·519 (5) | 2·511 (4) |
| *M*(32)—O(12) | 2·790 (10) | 2·792 (8) | 2·781 (7) |
| *M*(32)—O(21$^{ii}$) × 2 | 2·306 (4) | 2·312 (3) | 2·311 (3) |
| *M*(32)—O(31) × 2 | 2·433 (4) | 2·407 (3) | 2·386 (3) |
| *M*(32)—O(33) × 2 | 2·564 (4) | 2·551 (3) | 2·528 (2) |
| Mean | 2·485 (5) | 2·476 (4) | 2·462 (3) |
| *M*(4)—O(31$^{iii}$) × 2 | 2·399 (3) | 2·400 (2) | 2·396 (2) |
| *M*(4)—O(32$^{ii}$) × 2 | 2·331 (4) | 2·326 (4) | 2·320 (3) |
| *M*(4)—O(33$^{iii}$) × 2 | 2·349 (4) | 2·343 (3) | 2·339 (3) |
| Mean | 2·360 (4) | 2·356 (3) | 2·352 (3) |

Symmetry operations: (i) $y, x, -z$; (ii) $-y, x-y, z+\frac{1}{3}$; (iii) $-x+y, -x, z+\frac{2}{3}$; (iv) $-x, -x+y, -z+\frac{1}{3}$; (v) $x-y, -y, -z+\frac{2}{3}$.

* See the previous paper (Ohsato, Takéuchi & Maki, 1986) for the room-temperature data.

In $Na_6Ca_3[Si_6O_{18}]$ the bridging O atom was split into two because of the fairly large $B_{eq}$ (Ohsato, Maki & Takéuchi, 1985). In the high-temperature form of $Na_4Ca_4[Si_6O_{18}]$, the $B_{eq}$ for the bridging O atom, though larger than those for other O atoms, is not so large as to suggest the split model.

### *Rearrangement of* Na *and* Ca *ions upon transition*

Fig. 3 compares the six-membered $[Si_6O_{18}]^{12-}$ rings of the high- and low-temperature forms, each projected along the trigonal *c* axis and shown together with surrounding cations. The *M*(2) site in the high-temperature form is statistically occupied by Na ions and vacancies. Upon transition to the low-temperature form, the *M*(2) site is differentiated into two independent sites; *M*(21) is fully occupied by Na ions while *M*(22) is totally vacant as mentioned before (Fig. 3*b*). In the $Na_4Ca_4[Si_6O_{18}]$–$Na_6Ca_3[Si_6O_{18}]$ solid-solution series, excess Na ions, introduced by the replacement of Ca with 2Na, can be accommodated in the *M*(22) site which is entirely vacant in $Na_4Ca_4[Si_6O_{18}]$. The *M*(3) site, with 29% Na and 71% Ca ions, is also differentiated into *M*(31) and *M*(32); the former consists of 43% Na and 57% Ca ions and the latter exclusively of Ca ions.

Divalent Ca ions on *M*(32) lie preferentially around the vacant *M*(22) sites in conformity with the rule of maximal charge neutrality. The *M*(22) and *M*(32) sites form double spirals at intervals of *c*/2 around the threefold screw axes which intersect with the twofold axes and pass through the origin. In a similar way *M*(21) forms double spirals together with *M*(31) around the screw axes at $\frac{1}{3}, \frac{2}{3}, z$ and $\frac{2}{3}, \frac{1}{3}, z$ which do not intersect with the twofold axes.

No significant change in cationic occupancy occurs for *M*(1) and *M*(4) upon transition.

### *Deformation of coordination polyhedra*

The coordination polyhedron around *M*(1) in the high-temperature form has the shape of a distorted octahedron with a coordination number of six. Upon transition to the low-temperature form the *M*(1) site splits into two, producing a new additional site,

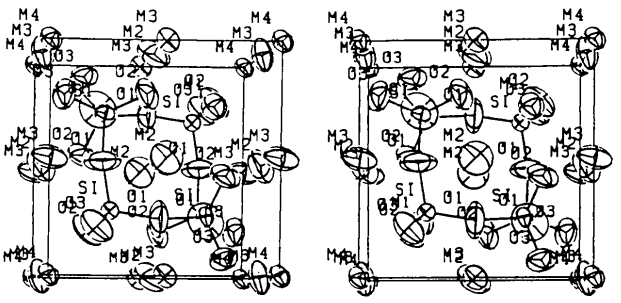


Fig. 2. Stereoscopic drawing of the rhombohedral unit-cell structure viewed along [001] at 773 K (*ORTEP*, Johnson, 1965).

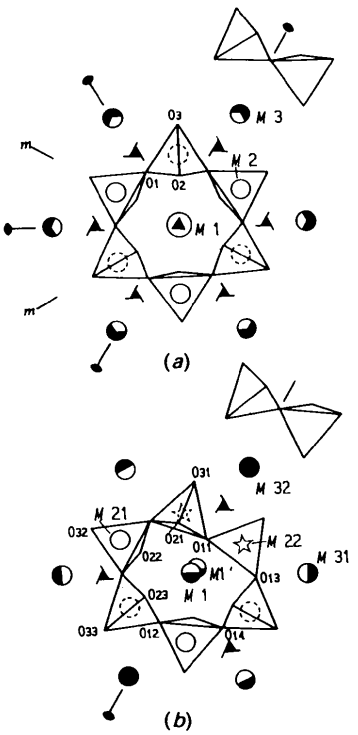


Fig. 3. Cation distribution and configuration of the $[Si_6O_{18}]^{12-}$ ring in (*a*) high- and (*b*) low-temperature forms.

$M(1')$, which is closer to the centre of the ring than $M(1)$ (Fig. 3). The separation between $M(1)$ and $M(1')$ at 738 K, for example, is 0·564 Å. This splitting of the $M(1)$ site is caused by the deformation of the ring as will be described later. Since the bridging O(11) atom shifts considerably towards the centre of the ring (Fig. 3), $M(1')$ has an additional neighbour at a distance 3·132 Å (738 K). $M(21)$, as well as $M(2)$, lies near the centre of the pseudocubic subcells and gives no appreciable change in coordination upon transition.

The coordination polyhedron having the shape of a hexagonal bipyramid for $M(3)$ becomes a distorted pentagonal bipyramid for both $M(31)$ and $M(32)$ with the reduction of coordination number from eight to seven. O(31) is omitted from the coordination polyhedron around $M(31)$ because of the lengthening of the $M(31)$—O(31) bond to 3·29 Å (738 K) owing mainly to the noticeable shift of O(11) towards the centre of the ring (Fig. 3). The $M(32)$—O(11) bond is also lengthened to 3·44 Å (738 K) owing to the shift of O(11). The regular octahedron around $M(4)$ in the high-temperature form is distorted slightly without change in coordination number.

Here it is noteworthy that Na ions enter into larger coordination polyhedra than Ca ions. The mean $M$—O bond length (523 K) is 2·62 Å for $M(21)$, which is occupied exclusively by Na ions; in contrast, it is 2·46 Å for $M(32)$ and 2·35 Å for $M(4)$, both being exclusively occupied by Ca ions. For $M(1)$ and $M(31)$, which are occupied by both Na and Ca ions (Table 2), the mean bond lengths are of intermediate value (2·47 and 2·51 Å, respectively). A similar trend has been reported by Takéuchi, Nishi & Maki (1980) for the $M$—O bond lengths in Na-doped tricalcium aluminate ($Na_xCa_{9-x/2}[Al_6O_{18}]$).

*Deformation of the six-membered ring*

The configurational change of the ring with temperature can be described in terms of the Si—O—Si angles (Fig. 4). In the high-temperature form all the angles are uniformly 163° and the six-membered ring bears a symmetrical form (Fig 3*a*). This situation presumably results from all the bridging O(1) atoms being coordinated by cations [$M(2)$ and $M(3)$] in a similar way. In the low-temperature form the Si—O—Si angles take diverse values ranging from 144 to 176°. In this form, both $M(2)$ and $M(3)$ are differentiated into two sites with different cationic occupancies. Among those cation sites, $M(22)$ is entirely vacant and $M(32)$ is no longer coordinated by O(11). In fact, O(11) shifts from its corresponding position in the high-temperature form towards the centre of the ring by 0·8 Å with the resultant change in the Si—O(11)—Si angle to *ca* 150°. This angle is close to the average value of 140° for the Si—O—Si angle in silicate structures (Liebau, 1985). On the other hand, the angle shows a value as large as 175° around O(12) which lies opposite to O(11) across the centre of the ring.

The mean bond lengths between Si and bridging and non-bridging O atoms of the silicate tetrahedra are shown as a function of temperature in Fig. 5. It is notable that the mean Si—O bond length is significantly shortened with increase of temperature. Such an experimental fact has also been observed for forsterite (Takéuchi, Yamanaka, Haga & Hirano, 1984).

The phase transition is thus characterized by change in cation distribution with concomitant configurational change of the ring. The structural change in the series $Na_4Ca_4[Si_6O_{18}]$–$Na_6Ca_3[Si_6O_{18}]$ can likewise be characterized by the change in distribution of cations, including vacancies, with the accompanying configurational change of the ring. More extensive structural studies on the solid-

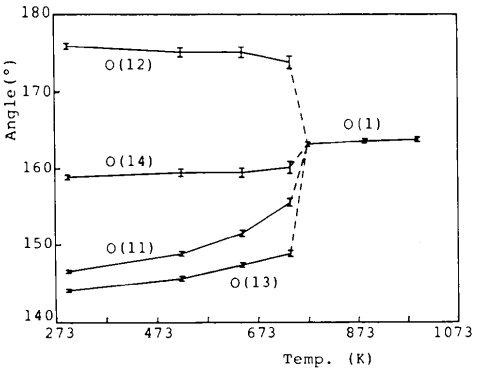


Fig. 4. Si—O—Si bond angles of the six-membered ring as a function of temperature. Vertical lines give e.s.d.'s.

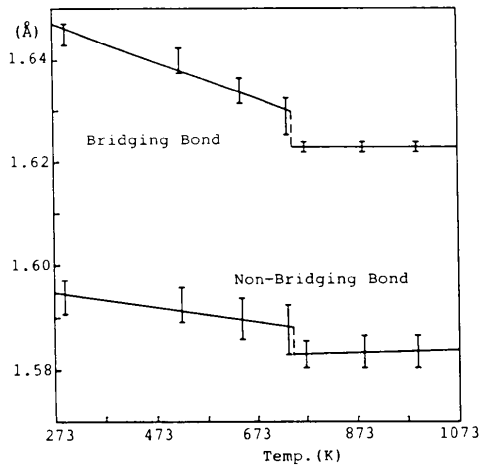


Fig. 5. Mean bond lengths of Si—O as a function of temperature. Vertical lines give e.s.d.'s.

solution series are desirable for elucidating further details of the phase transition.

We would like to thank Professors H. Minato and T. Sugimura for helpful suggestions, Drs N. Haga and F. Nishi for valuable discussions and Mr K. Oyobe for his assistance in drawing the figures. We thank the Ministry of Education, Science and Culture for supporting the leave of HO to carry out this work for a year at the Mineralogical Institute, Faculty of Science, University of Tokyo.

### References

BOND, W. L. (1951). *Rev. Sci. Instrum.* **22**, 344–345.
BROWN, G. E., SUENO, S. & PREWITT, C. T. (1973). *Am. Mineral.* **58**, 619–697.
BUSING, W. R., MARTIN, K. O. & LEVY, H. A. (1963). *RADY.* Report ORNL-TM-305. Oak Ridge National Laboratory, Tennessee, USA.
FISCHER, R. X. & TILLMANNS, E. (1983). *Neues Jahrb. Mineral. Monatsh.* **2**, 49–59.
FISCHER, R. X. & TILLMANNS, E. (1984). *Z. Kristallogr.* **166**, 245–256.
FISCHER, R. X. & TILLMANNS, E. (1987). *Acta Cryst.* C**43**, 1852–1854.
IKAWA, H., OTAGIRI, T., IMAI, O., SUZUKI, M., URABE, K. & UDAGAWA, S. (1986). *J. Am. Ceram. Soc.* **69**, 492–498.
*International Tables for X-ray Crystallography* (1974). Vol. IV. Birmingham: Kynoch Press. (Present distributor Kluwer Academic Publishers, Dordrecht.)
JOHNSON, C. K. (1965). *ORTEP.* Report ORNL-3794. Oak Ridge National Laboratory, Tennessee, USA.
LIEBAU, F. (1985). *Structural Chemistry of Silicates,* pp. 24–30. Berlin: Springer-Verlag.
MAKI, I. & SUGIMURA, T. (1968). *Yogyo Kyoukai Shi,* **76**, 144–148.
OHSATO, H., MAKI, I. & TAKÉUCHI, Y. (1985). *Acta Cryst.* C**41**, 1575–1577.
OHSATO, H., TAKÉUCHI, Y. & MAKI, I. (1986). *Acta Cryst.* C**42**, 934–937.
TAKÉUCHI, Y., NISHI, F. & MAKI, I. (1980). *Z. Kristallogr.* **152**, 259–307.
TAKÉUCHI, Y., YAMANAKA, T., HAGA, N. & HIRANO, M. (1984). *Materials Science of the Earth's Interior,* edited by I. SUNAGAWA, p. 191 Tokyo: Terrapub.
TAYLOR, D. (1984). *Mineral. Mag.* **48**, 65–79.
TOKONAMI, M. (1965). *Acta Cryst.* **19**, 486.

*Acta Cryst.* (1990). B**46**, 131–138

# Structure, Electron Density and Thermal Motion of $KCuF_3$

BY R. H. BUTTNER, E. N. MASLEN AND N. SPADACCINI

*Department of Physics, University of Western Australia, Nedlands, WA* 6009, *Australia*

(*Received* 30 *January* 1989; *accepted* 9 *October* 1989)

## Abstract

Thermal parameters from a refinement with newly collected data for $KCuF_3$ [$M_r = 159{\cdot}64$, tetragonal, $I4/mcm$, $a = b = 5{\cdot}8569\ (6)$, $c = 7{\cdot}8487\ (8)$ Å, $V = 269{\cdot}24\ (6)$ Å$^3$, $Z = 4$, $D_x = 3{\cdot}938$ Mg m$^{-3}$, $\lambda$(Mo $K\alpha$) $= 0{\cdot}71069$ Å, $\mu = 9{\cdot}747$ mm$^{-1}$, $F(000) = 300$, $T = 298$ K, final $R = 0{\cdot}020$, $wR = 0{\cdot}014$ for 655 unique reflections] are consistent with those from a reanalysis of previously published data with a revised model including an isotropic extinction correction. There are two distinct types of F atoms and three different Cu—F bonds. The amplitude of the Cu—F2 stretching mode is largest for the long Cu—F2 bond. The single refined positional parameter differs significantly from previous determinations but the difference is shown to be due to bias in the redistribution of bonding electron density. Its value from refinement with full data gives a more satisfactory description of the net force at equilibrium geometry than that based on high-angle refinement. Effective atomic charges for Cu, K and F2, calculated by partitioning the difference density, are consistent with those in related structures but F1 is positively charged. This is explained by the strong depleting effect of exchange on the electron density, owing to structural compression along the $c$ axis. The positive charge on F1 accounts for changes in K—F and F—F distances from the ideal perovskite values. There is excess electron density of $1{\cdot}61$ e Å$^{-3}$ located $0{\cdot}45$ Å from F2, indicating strong dipole polarization along the Cu—F2—Cu bond. The shape of the depletion of electron density near Cu is broadly compatible with that expected for a cooperative Jahn–Teller distorted Cu system, but its radial dependence suggests depletion of paired spins along the shorter Cu—F bonds and of unpaired spins along the longest Cu—F bond.

## Introduction

$KCuF_3$ contains atoms with moderate atomic number enabling its electron density to be measured

0108-7681/90/020131-08$03.00